

Subdiffusive front scaling in interacting integrable models

Vir B. Bulchandani¹ and Christoph Karrasch²

¹*Department of Physics, University of California, Berkeley, Berkeley CA 94720, USA*

²*Dahlem Center for Complex Quantum Systems and Fachbereich Physik,
Freie Universität Berlin, 14195 Berlin, Germany*

(Dated: July 22, 2022)

In the wake of theoretical advances in the understanding of ballistic transport in interacting integrable models, there has been an increased focus on subleading corrections to ballistic behaviour. Recently, the leading diffusive term in the hydrodynamics of such models was derived and shown to be non-zero in general. At the same time, numerical evidence for superdiffusive spin transport in the spin-1/2 Heisenberg model suggests that richer dynamical behaviours may also occur. The purpose of the present work is to show that any interacting integrable model possesses a class of initial states for which the leading corrections to ballistic hydrodynamics are subdiffusive rather than diffusive, indicating that “anomalous” dynamics, i.e. that which is neither ballistic nor diffusive, is more widespread in such models than is usually assumed. These initial states are natural to realize experimentally and include the domain wall initial condition that has been the object of much recent scrutiny. Upon performing numerical matrix product state simulations in the spin-1/2 XXZ chain, we find that such states can exhibit subdiffusive $t^{1/3}$ scaling of fronts of spin, energy and entanglement entropy across the entire range of anisotropies. This demonstrates that “Tracy-Widom” scaling is not incompatible with model interactions, as was previously believed.

Introduction The typical relaxation dynamics of conserved quantities such as energy and particle number in classical many-body systems has been understood for well over a century, and is described to a great degree of accuracy by phenomenological “laws of diffusion”, such as Fick’s law and Fourier’s law. At the same time, attempts to derive these laws from a microscopic model of deterministic Hamiltonian evolution are still in their infancy, owing to the tremendous technical difficulties involved in such a task¹. These difficulties are perhaps related to a growing understanding that classical transport in low dimensions is frequently *anomalous*, in the sense of being characterized by quantities that exhibit $t^{1/3}$ scaling with time^{2,3} corresponding to the KPZ universality class of dynamics, rather than ordinary, microscopic Brownian motion that would give rise to diffusive $t^{1/2}$ scaling.

These recent advances in the theory of low-dimensional classical transport have been complemented by the development of a hydrodynamic theory of time-evolution in quantum integrable models^{4,5}, which usually goes by the name of “generalized hydrodynamics”. Quantum integrable models include experimentally realizable examples like the Lieb-Liniger gas of delta interacting bosons in one spatial dimension and the spin-1/2 Heisenberg chain. At first, generalized hydrodynamics was limited to describing ballistic transport in such models, for which it has so far yielded impressive agreement with numerical simulations^{4–14}. However, the diffusive corrections to the “Bethe-Boltzmann” equation underlying the hydrodynamic approach were recently derived^{15,16}, and have raised the novel possibility of using generalized hydrodynamic techniques to analyze sub-leading corrections to ballistic transport.

In the present work, we study time-evolution from a class of initial states in the spin-1/2 XXZ chain with

anisotropy Δ , for which these recent results predict that the diffusive corrections to the Bethe-Boltzmann equation ought to vanish. Upon performing numerical simulations using the real-time density matrix renormalization group^{17–19}, we find that these states exhibit subdiffusive $t^{1/3}$ scaling of fronts of spin, energy and entanglement entropy across the entire range of anisotropies, which we interpret to be a consequence of third-order hydrodynamic effects²⁰ in the propagating front. The class of states we discuss includes a domain-wall initial state that was found to support superdiffusive transport at the isotropic point^{21,22} $\Delta = 1$; it was subsequently argued that this effect might be a transient deviation from diffusive transport²³. The fact that the leading corrections to ballistic transport are diffusive away from the isotropic point is supported by studies of domain-wall initial states in the gapless phase, $|\Delta| < 1$, including a hydrodynamic argument¹³ that fronts of spin scale with time as $t^{1/2}$, together with an analytical study of return probabilities in the six-vertex model that also found the $t^{1/2}$ scaling characteristic of diffusion²⁴.

Before presenting our results in detail, we briefly summarize how they relate to these earlier analyses of time evolution from domain-wall initial states. For time evolution from domain walls with $|\Delta| < 1$, we find that ballistic fronts of spin and energy propagate at a light-cone speed $v_* = 1$, rather than the value $v_* = \sqrt{1 - \Delta^2}$ found in previous works^{13,24}. Spreading of observables in the “forbidden” region $\sqrt{1 - \Delta^2} < x/t < 1$ was explicitly noted in Ref. [24] (and indeed earlier²¹), but characterized as a transient effect. Here, we argue that this discrepancy with theory is due to a specific choice of “coarse-graining” in earlier works, corresponding to the ansatz Eq. (9) for the hydrodynamic initial state, which omits the finite energy density at the domain wall itself

and so cannot provide an exact description of the dynamics on accessible (non asymptotic) time scales. Upon performing a scaling analysis of tDMRG data at the physical light-cone edge, we find $t^{1/3}$ behaviour rather than diffusive $t^{1/2}$ scaling; an example is shown in Fig. 2. Conventional wisdom also predicts a vanishing ballistic contribution to time-evolution from domain walls with $\Delta \geq 1$, again based on the “two-reservoir” hydrodynamic ansatz, Eq. (9). By contrast, we find that the domain wall carries an effective, localized energy $\delta E = -J\Delta/2$ for all values of the anisotropy Δ , which spreads ballistically through the system even for $\Delta \geq 1$. From numerical tDMRG simulations, we find that these energy fronts are accompanied by ballistically spreading fronts of spin and entanglement entropy, and that the corrections to ballistic behaviour for all of these quantities scale as $t^{1/3}$. See Fig. 1 for examples with $\Delta > 1$, or the Appendix for examples with $\Delta = 1$.

Hydrodynamics of integrable models. Consider a generic quantum integrable model, whose equilibrium states may be characterized in terms of quasiparticle distribution functions $\rho_{n,k}$, with $n \in \mathbb{N}$ a discrete quasiparticle index and $k \in \mathbb{R}$ a continuous rapidity variable. There is now a substantial body of numerical evidence^{4–14} that the ballistic part of time-evolution in such models, from smooth, locally equilibrated initial conditions, i.e. those that can be modelled by smoothly varying distribution functions $\rho_{n,k}(x)$, may be captured by the system of Boltzmann-type equations^{4,5}

$$\partial_t \rho_{n,k} + \partial_x (\rho_{n,k} v_{n,k}[\rho]) = 0, \quad (1)$$

where the local quasiparticle velocities $v_{n,k}(x, t)$ at each space-time point are fixed in terms of the full set of local distribution functions $\{\rho_{n',k'}(x, t) : n' \in \mathbb{N}, k' \in \mathbb{R}\}$ via thermodynamic Bethe ansatz. As it stands, the system (1) conserves the local Yang-Yang entropy density at each point (as follows from its time-reversal invariance) and so cannot capture diffusive effects. However, the leading diffusive correction to this ballistic hydrodynamics was recently derived by taking two-body scattering processes into account¹⁵ and upon including this correction, the entropy-conserving system (1) is replaced by a dissipative system of equations, of the form

$$\partial_t \rho_{n,k} + \partial_x (\rho_{n,k} v_{n,k}[\rho]) = \partial_x (\mathcal{D}_{n,k}[\partial_x \rho]). \quad (2)$$

where the “diffusion operator” $\mathcal{D}_{n,k}$ acts on $\partial_x \rho$ as a linear integral kernel. Meanwhile, a kinetic theory argument based on the propagation of a tagged soliton through a fluctuating medium¹⁶ predicts the linear diffusion equation

$$\partial_t \delta \theta_{n,k} + v_{n,k}[\theta] \partial_x \delta \theta_{n,k} = D_{n,k}[\theta] \partial_{xx} \delta \theta_{n,k} \quad (3)$$

for small perturbations $\delta \theta_{n,k}(x, t)$ of a locally equilibrated background with local Fermi factors $\{\theta_{n',k'}(x, t) :$

$n' \in \mathbb{N}, k' \in \mathbb{R}\}$. This turns out to coincide with the diagonal, linear-response component of the full transport equation Eq. (2), as might be expected from its derivation²⁵. In the present work, our arguments are based on the qualitative picture leading to Eq. (3) but our conclusions are also consistent with the full transport equation, Eq. (2).

Diffusive vs subdiffusive corrections to hydrodynamics. For non-interacting integrable models, in the sense of Ref. [26], the possibility of subdiffusive $t^{1/3}$ scaling of ballistic fronts is well-established by now^{27–30}, and was recently given a new interpretation as an effect in “third-order hydrodynamics”²⁰, which is characterized by the absence of diffusive terms. By contrast, a recently discovered link between linear-response diffusive corrections to the Bethe-Boltzmann equation and local density fluctuations¹⁶ indicates that for locally equilibrated states of interacting integrable models, the generic scaling of operator fronts goes as $t^{1/2}$, rather than $t^{1/3}$. The key insight is that the density fluctuations giving rise to microscopic diffusion are controlled by fluctuations $\delta \theta_{n,k}$ in the local Fermi factors, which satisfy³¹

$$\langle \delta \theta_{n,k} \delta \theta_{n',k'} \rangle \propto \delta_{n,n'} \delta(k - k') \theta_{n,k} (1 - \theta_{n,k}) \quad (4)$$

on a given interval. In order for diffusive corrections to vanish, the Fermi factors $\theta_{n,k}$ must vanish for all n and k at every space-time point. Thus, as claimed in Ref. [16], a generic local equilibrium state of an interacting integrable model will exhibit diffusive corrections to ballistic dynamics, and consequently $t^{1/2}$ scaling of operator fronts. The observation that we wish to make in the present work is that the “exceptional case” for which there is vanishing entropy production in the majority of the system, or equivalently, for which $\theta_{n,k}$ is 0 or 1 almost everywhere, is physically rather natural. For example, in the context of spin-1/2 XXZ chains, this class of states encompasses any initial condition that consists of macroscopically large ferromagnetic domains with spin alignment along the z -axis, which are simple to realize experimentally in spin-chain compounds³². Similar zero-entropy initial states were considered in the context of Lieb-Liniger Bose gases⁹. On the basis of the formula Eq. (4) and recent theoretical results on third-order hydrodynamics²⁰, we conjecture that for any integrable lattice model with nearest-neighbour interactions, initial states that are “pseudo-vacua” in bulk will support $t^{1/3}$ corrections to ballistic dynamics, provided that the bare dispersion of the fastest quasiparticle satisfies the technical conditions discussed in Ref. [20]. The single magnon excitation in the spin-1/2 XXZ chain satisfies these conditions³³ for all values of the anisotropy Δ , allowing for a direct test of our predictions against matrix product state numerical simulations.

Upon performing a scaling analysis of tDMRG data for spin, energy and single-cut entanglement entropy in two classes of such initial states in the spin-1/2 XXZ

chain, namely i) domain wall initial conditions, which have come under recent scrutiny^{13,22–24} and ii) initial conditions consisting of a single flipped down spin in a sea of up spins, we find evidence for $t^{1/3}$ scaling of fronts across the entire anisotropy range of the XXZ chain. In more detail, for the initial condition (i) with $\Delta \geq 1$, we find that the single-cut entanglement entropy at a point x exhibits front scaling

$$S_E(x, t) \sim t^{-1/3} f\left(\frac{x-t}{t^{1/3}}\right), \quad (5)$$

consistent with the usual Airy kernel^{27–29} (see Fig. 1), while for both initial conditions (i) and (ii) and all anisotropies Δ , fronts of spin and energy exhibit the scaling form

$$\delta\langle\mathcal{O}\rangle(x, t) \sim t^{-2/3} g\left(\frac{x-t}{t^{1/3}}\right), \quad (6)$$

reminiscent of the derivative of the Airy kernel (see Fig. 2 and Appendix) that was found to capture front-scaling in the critical transverse-field Ising chain³⁰. A detailed analysis of this phenomenon is beyond the scope of the present work, though some analytical results for the spin-flip initial condition are summarized in the Appendix.

Initial states supporting subdiffusion of fronts. We now discuss the initial conditions (i) and (ii) in more detail. The Hamiltonian under consideration is the spin-1/2 XXZ chain with anisotropy Δ , namely

$$H = J \sum_{i=1}^L S_i^x S_{i+1}^x + S_i^y S_{i+1}^y + \Delta S_i^z S_{i+1}^z. \quad (7)$$

The first class of initial states we consider has the form

$$|\psi\rangle = |\uparrow\rangle^{\otimes L/2} \otimes |\downarrow\rangle^{\otimes L/2}. \quad (8)$$

This initial condition has been studied frequently in recent works, both at the isotropic point^{22,23} $\Delta = 1$ and in the gapless phase^{13,24} of the XXZ model. At this point, a remark on the applicability of hydrodynamics to the domain wall initial state is in order. In principle, hydrodynamics is only valid for smooth, locally equilibrated initial conditions. This assumption is crucial because in order to apply Eq. (1) or Eq. (2), the description of the initial state in terms of local quasiparticle distribution functions $\rho_{n,k}(x)$ must be well-defined. This makes hydrodynamics an ideal tool for studying, say, time-evolution from density matrices of the form $\rho = e^{-\sum_j \beta_j h_j} / Z$, with β_j varying slowly with j . By contrast, a ferromagnetic domain wall can be regarded as smooth and locally stationary everywhere except at the domain wall itself. In most situations, this would be a minor technical point that does not affect dynamics in the ballistic scaling limit, for which hydrodynamics

probably yields an exact description. However, for a ferromagnetic domain wall, the usual prescription of writing the initial state as

$$\theta_{n,k}(x) = \begin{cases} \theta_{n,k}^L(x) & x \leq 0 \\ \theta_{n,k}^R(x) & x > 0 \end{cases}, \quad (9)$$

where $\theta^{L/R}$ describe the bulk equilibrium states on either side of the domain wall, seems to us to be overly simplistic. The reason is that the domain wall itself has energy offset $\delta E = -J\Delta/2$ compared to the background energy density $h(x, t) = J\Delta/4$, and this offset spreads ballistically through the system on accessible time scales. By contrast, the initial condition (9) (which amounts to a specific choice of coarse-graining protocol), excludes the fluid cell that actually contains the domain wall, and therefore misses this finite energy.

This issue becomes especially clear for $|\Delta| \geq 1$, where the naive hydrodynamic description of the initial state³⁴, Eq. (9), is everywhere zero, as follows from the formula¹¹

$$|\langle s_z \rangle| = \frac{1}{2} - \sum_{n=1}^{\infty} \int d\lambda n \rho_{n,\lambda}. \quad (10)$$

One could argue that the “freezing” of dynamics in the gapped phase^{35,36} is perfectly consistent with such an initial state. However, for all $\Delta \geq 1$ we find clear numerical evidence for ballistic spreading of entanglement (see Fig. 1) accompanied by a small amount of ballistically spreading spin and energy (see Appendix), suggesting that Eq. (9) is incomplete as it stands. Moreover, a hydrodynamic coarse graining that omits $x = 0$ would predict precisely the same hydrodynamic evolution for the initial state

$$|\psi\rangle = |\uparrow\rangle^{\otimes L/2-1} \otimes |\downarrow\rangle \otimes |\uparrow\rangle^{\otimes L/2}, \quad (11)$$

even though the latter initial state is not “frozen” and would be expected to exhibit ballistic transport of spin and energy. In both cases, a prerequisite for an accurate hydrodynamic description of the initial state is a correct treatment of the fluid cell at $x = 0$.

Putting such subtleties aside for the moment, let us focus on the key physical feature that the states (8) and (11) have in common, namely that the occupation numbers on either side of the “defect” at $x = 0$ are zero (with respect to the bulk). For both initial states, the defect creates counter-propagating pairs of magnons (and possibly higher strings as well) that spread into the bulk pseudo-vacua on either side. Since there is no velocity dressing, and according to Eq. (4), density fluctuations of the background vanish, the kinetic theory argument of Ref. [16] indicates that the leading-order correction to ballistic hydrodynamics occurs at third-order in a derivative expansion. In particular, near the edge of the front where magnons are the only propagating degrees of freedom, the third-order hydrodynamic equation discussed in

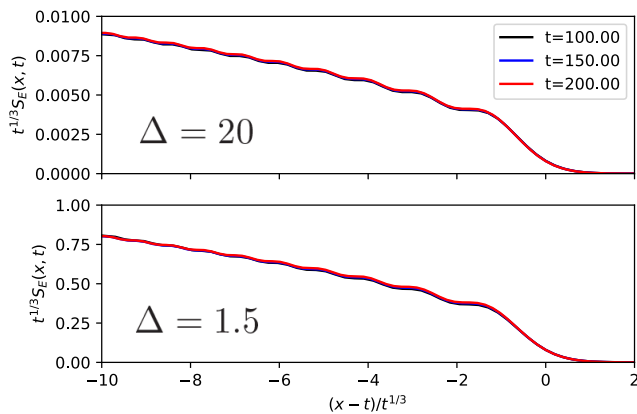


FIG. 1. Scaling of fronts of the single-cut entanglement entropy in tDMRG data for time-evolution from domain wall initial conditions in the gapped phase of the XXZ chain, with example anisotropies $\Delta = 1.5$ and $\Delta = 20$. The $t^{1/3}$ scaling collapse, together with the “staircase feature” characteristic of the Airy kernel, are clear.

Ref. [20] should apply (indeed, a non-trivial consistency check on integrable hydrodynamics is that it reduces to free-particle hydrodynamics in the absence of quasiparticle dressing). Based on this observation, we expect that the leading corrections to the ballistic front scale as $t^{1/3}$ for both the initial conditions (8) and (11), and below we confirm this hypothesis by direct comparison with numerical tDMRG simulations.

$\Delta \geq 1$: *domain-wall initial conditions.* As discussed above, the localized initial energy density at $x = 0$ gives rise to ballistic quasiparticle spreading even in the regime $\Delta \geq 1$. A particularly clear way to see this is from the single-cut entanglement entropy, whose fronts propagate ballistically in time for all values of the anisotropy $\Delta \geq 1$, in a manner consistent with the creation of counter-propagating pairs of magnons at the domain wall itself³⁷ (this has already been noted²³ at $\Delta = 1$). Entanglement spreading from domain wall initial conditions in the gapped phase of the XXZ chain will be discussed further in related work³⁸ on the hydrodynamic approach to entanglement entropy^{39–42}. Upon plotting the fronts of single-cut entanglement entropy (as was previously done for free fermions²⁹), we find that entanglement fronts exhibit the $t^{1/3}$ scaling previously thought to be specific to non-interacting systems, together with the “staircase” feature characteristic of the Airy kernel^{27,29,30}. See Fig. 1.

$|\Delta| < 1$: *domain-wall initial conditions.* For $|\Delta| < 1$, evolution of entanglement from domain-wall initial conditions, as was considered above, exhibits non-ballistic growth in time due to the gaplessness of magnon excitations on each pseudo-vacuum. However, as for $\Delta \geq 1$, there is ballistic transport of spin and energy. To our surprise, the standard scaling analysis of spin fronts^{27,29}

does not appear clearly to distinguish between diffusive and subdiffusive scaling. We put this ambiguity down to the dominance of the ballistic part of transport and therefore subtract the “two-reservoir” hydrodynamic prediction for the steady-state spin density, given at roots of unity $\Delta = \cos \gamma$, $\gamma = \pi/\nu$, $\nu \in \{2, 3, \dots\}$, by^{13,24}

$$s_z^{hydro}(x, t) = \begin{cases} 0.5 & x < -(\sin \gamma)t \\ -\frac{1}{2\gamma} \sin^{-1}\left(\frac{x}{t}\right) & |x| < (\sin \gamma)t \\ -0.5 & x > (\sin \gamma)t \end{cases} \quad (12)$$

Once this is subtracted from the numerical data, the oscillatory features in the spin front show a marked collapse to $t^{1/3}$ rather than $t^{1/2}$ scaling; see Fig. 2 for an example with $\Delta = 0.5$. For the energy fronts, we merely subtract the bulk value $\langle h \rangle = J\Delta/4$ as usual²⁷, and observe the same scaling.

In both cases, our rescaled horizontal coordinate involves $x - t$, rather than the parameter $x - \sqrt{1 - \Delta^2}t$ plotted in previous work¹³. This is because on accessible time-scales, we observe that fronts of both spin and energy travel with a light-cone speed $v^* = 1$, which is consistent with the light-cone for single-magnon excitations on each pseudo-vacuum. One could treat the part of the spin front propagating faster than $v^* = \sqrt{1 - \Delta^2}$ as a finite-size effect, as was done in previous works^{13,24}. However, since the localized initial energy density of the domain wall is omitted from the hydrodynamic ansatz Eq. (9), and we observe numerically that energy spreads ballistically with light-cone speed $v^* = 1$ for all anisotropies Δ , we suspect that this discrepancy is due to the choice of coarse-graining at $x = 0$ that was discussed above. The same effect may be responsible for the poorly scaling region in the upper half of Fig. 2.

Decay of a single spin-flip. Finally, we consider evolution from an initial condition consisting of a single flipped spin at $x = 0$. Here, the bulk state has constant spin and energy densities $\langle s_z \rangle = 1/2$ and $\langle h \rangle = J\Delta/4$. Upon subtracting this background, we find $t^{1/3}$ scaling of spin and energy fronts for all anisotropies $\Delta \geq 0$. Of course, the single flipped spin has a simple description as a spatially localized superposition of magnons, so that $t^{1/3}$ front scaling can be derived directly from wavefunction asymptotics, as in the free-fermion case^{27,43}. This derivation is summarized in the Appendix. The novelty here is the connection with interacting domain wall initial states, via hydrodynamics.

Discussion. The above arguments indicate that the “exceptional” case of vanishing entropy production in locally equilibrated states of quantum integrable models¹⁶ in fact includes a class of states that arise quite naturally in practice, since any initial condition that gives rise to a dilute gas of quasiparticle excitations propagating through a bulk pseudo-vacuum will lack the local density fluctuations that generate diffusion. The absence of bulk entropy production in these states can also

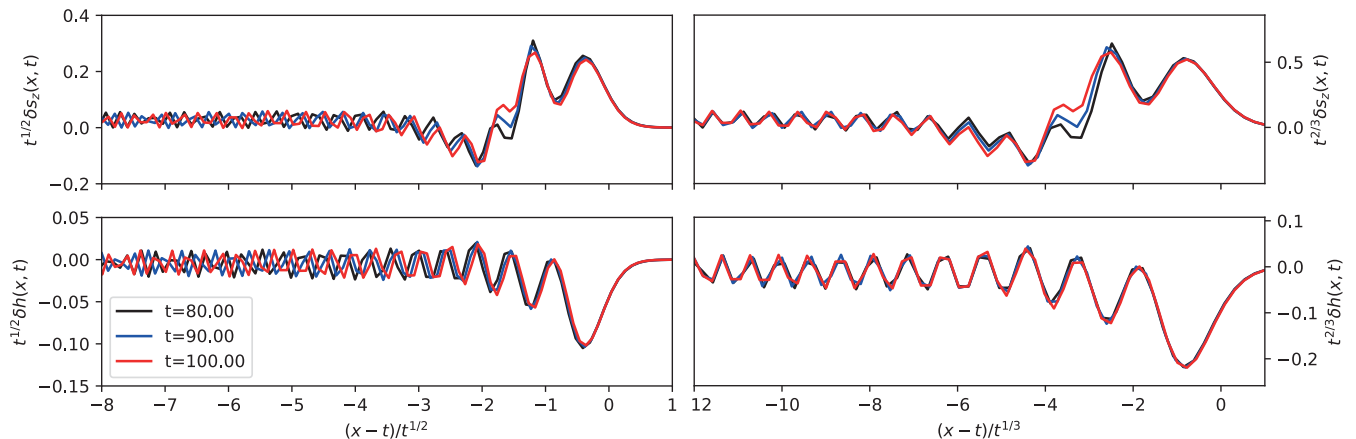


FIG. 2. Diffusive (*left*) versus subdiffusive (*right*) rescaling of fronts of spin (*top*) and energy (*bottom*), obtained from tDMRG predictions for time-evolution from domain wall initial conditions in the gapless phase of the XXZ chain, with anisotropy $\Delta = 0.5$. The improvement in scaling collapse for the right-hand figures is marked.

be seen from the vanishing of the diffusion kernel¹⁵ in the full transport equation, Eq. (2). Experimental realizations of such physics include the free expansion of a spatially localized initial density of Lieb-Liniger gas and, perhaps more surprisingly, the example of time-evolution from ferromagnetic domain walls in spin-1/2 XXZ chains that was discussed in detail above.

Furthermore, our analysis identifies the basic inadequacy of using “two-reservoir” type initial conditions, as in Eq. (9), to model certain types of initial state, including the mixed states

$$\rho = (\mathbb{1} + \mu\sigma^z)^{\otimes L/2} \otimes (\mathbb{1} - \mu\sigma^z)^{\otimes L/2} \quad (13)$$

that were shown to support superdiffusive spin transport at the isotropic point^{22,44} of the spin-1/2 XXZ chain (note that in this paper we studied the propagation of *fronts*, not transport properties). Previously, it was assumed that hydrodynamics could say nothing about time evolution from initial states such as (13) for $\Delta \geq 1$, because the initial condition Eq. (9) is homogeneous for these states. By contrast, our demonstration that an accurate hydrodynamic description of the state (13) at $\mu = 1$ needs to be augmented by initial data localized about $x = 0$ suggests that such a modification is also necessary for $\mu < 1$. At the same time, our results show that third-order effects can generate non-negligible corrections to ballistic dynamics, even in fully interacting integrable models. Whether or not these refinements of generalized hydrodynamics can shed any light not only on the scaling of fronts, but also on the rich variety of transport phenomena observed at the isotropic point^{21–23,44,45} of the XXZ chain, requires further investigation. Nonetheless, we hope that our results can motivate fresh approaches to the problem.

Acknowledgments We are grateful to Romain Vasseur, Joel E. Moore, Jacopo de Nardis, Benjamin

Doyon and Marko Žnidarič for their comments on the manuscript. We also thank Thomas Scaffidi and Xiangyu Cao for helpful discussions on related topics.

-
- [1] F. Bonetto, J. L. Lebowitz, and L. Rey-Bellet, .
 - [2] H. van Beijeren, *Physical Review Letters* **108**, 180601 (2012).
 - [3] H. Spohn, *Journal of Statistical Physics* **154**, 1191 (2014).
 - [4] O. A. Castro-Alvaredo, B. Doyon, and T. Yoshimura, *Physical Review X* **6**, 041065 (2016), arXiv:1605.07331.
 - [5] B. Bertini, M. Collura, J. De Nardis, and M. Fagotti, *Physical review letters* **117**, 207201 (2016), arXiv:1605.09790.
 - [6] E. Ilievski and J. De Nardis, *Physical Review Letters* **119** (2017), 10.1103/PhysRevLett.119.020602, arXiv:1702.02930.
 - [7] V. B. Bulchandani, R. Vasseur, C. Karrasch, and J. E. Moore, *Physical Review B* **97** (2018), 10.1103/PhysRevB.97.045407, arXiv:1702.06146.
 - [8] V. B. Bulchandani, R. Vasseur, C. Karrasch, and J. E. Moore, *Physical Review Letters* **119** (2017), 10.1103/PhysRevLett.119.220604, arXiv:1704.03466.
 - [9] B. Doyon, J. Dubail, R. Konik, and T. Yoshimura, *Phys. Rev. Lett.* **119**, 195301 (2017).
 - [10] E. Ilievski and J. De Nardis, *Physical Review B* **96**, 081118 (2017), arXiv:1706.05931.
 - [11] L. Piroli, J. De Nardis, M. Collura, B. Bertini, and M. Fagotti, *Physical Review B* **96** (2017), 10.1103/PhysRevB.96.115124, arXiv:1706.00413.
 - [12] V. Alba, *Physical Review B* **97**, 1 (2018), arXiv:1706.00020.
 - [13] M. Collura, A. De Luca, and J. Viti, *Physical Review B* **97**, 081111 (2018).
 - [14] A. Urichuk, Y. Oez, A. Klümper, and J. Sirker, (2018), arXiv:1808.09033.

- [15] J. De Nardis, D. Bernard, and B. Doyon, (2018), arXiv:1807.02414.
- [16] S. Gopalakrishnan, D. A. Huse, V. Khemani, and R. Vasseur, (2018), arXiv:1809.02126.
- [17] S. R. White and A. Feiguin, Phys. Rev. Lett. **93**, 076401 (2004).
- [18] U. Schollwoeck, Annals of Physics **326**, 96 (2011), january 2011 Special Issue.
- [19] C. Karrasch, J. E. Moore, and F. Heidrich-Meisner, Physical Review B **89**, 075139 (2014).
- [20] M. Fagotti, Physical Review B **96**, 220302 (2017).
- [21] D. Gobert, C. Kollath, U. Schollwöck, and G. Schütz, Phys. Rev. E **71**, 036102 (2005).
- [22] M. Ljubotina, M. Žnidarič, and T. Prosen, Nature Communications **8** (2017), 10.1038/ncomms16117, arXiv:1702.04210.
- [23] G. Misguich, K. Mallick, and P. L. Krapivsky, Physical Review B **96**, 195151 (2017).
- [24] J.-M. Stéphan, Journal of Statistical Mechanics: Theory and Experiment **2017**, 103108 (2017).
- [25] To be specific, the derivation of Eq. (3) considers perturbations only in the channel with quasiparticle index n and rapidity k , and neglects any back-reaction effects that would generate off-diagonal couplings to indices $n' \neq n$ or rapidities $k' \neq k$. Such back-reaction effects are taken into account by the full transport equation Eq. (2), but the conclusions of the present work appear to be insensitive to these corrections.
- [26] H. Spohn, Journal of Mathematical Physics **59**, 091402 (2018).
- [27] V. Hunyadi, Z. Rácz, and L. Sasvári, Physical Review E **69**, 066103 (2004).
- [28] T. Platini and D. Karevski, The European Physical Journal B - Condensed Matter and Complex Systems **48**, 225 (2005).
- [29] V. Eisler and Z. Rácz, Physical Review Letters **110**, 060602 (2013), arXiv:1211.2321.
- [30] M. Kormos, SciPost Phys. **3**, 020 (2017).
- [31] P. Fendley and H. Saleur, Physical Review B - Condensed Matter and Materials Physics **54**, 10845 (1996), arXiv:9601117 [cond-mat].
- [32] A. V. Sologubenko, T. Lorenz, H. R. Ott, and A. Freimuth, Journal of Low Temperature Physics **147**, 387 (2007).
- [33] This is immediate from its cosine dispersion and full pseudomomentum range. In fact, for $\Delta \geq 1$ it is additionally true for *all* string excitations, for the same reason⁴⁶.
- [34] The sign of the magnetization¹¹ is one way to specify the initial state more precisely but is not directly relevant to the physical phenomena under discussion here, since our remarks apply to energy as well as spin.
- [35] I. G. Gochev, Sov. Phys. JETP **58**, 115 (1983).
- [36] J. Mossel and J.-S. Caux, New Journal of Physics **12**, 055028 (2010).
- [37] More precisely, for $\Delta \gtrsim 5$, the domain wall seems to excite only single-magnon excitations, while as $\Delta \rightarrow 1$, higher strings are also excited.
- [38] V. B. Bulchandani, T. Scaffidi, C. Karrasch, and R. Vasseur, in preparation.
- [39] P. Calabrese and J. Cardy, Journal of Statistical Mechanics: Theory and Experiment **2005**, P04010 (2005).
- [40] V. Alba and P. Calabrese, Proceedings of the National Academy of Sciences of the United States of America **114**, 7947 (2017).
- [41] V. Alba, Physical Review B **97**, 1 (2018), arXiv:1706.00020.
- [42] B. Bertini, M. Fagotti, L. Piroli, and P. Calabrese, Journal of Physics A: Mathematical and Theoretical **51**, 39LT01 (2018).
- [43] T. Antal, Z. Rácz, A. Rákos, and G. M. Schütz, Physical Review E **59**, 4912 (1999).
- [44] M. Žnidarič, Physical Review Letters **106**, 220601 (2011).
- [45] M. Ljubotina, M. Žnidarič, and T. Prosen, Journal of Physics A: Mathematical and Theoretical **50**, 475002 (2017).
- [46] M. Takahashi, *Thermodynamics of One-Dimensional Solvable Models* (Cambridge University Press, 1999).

Front-scaling for domain wall initial conditions at $\Delta = 1$

In this appendix, we include figures for the scaling of the ballistically spreading fronts of entanglement (Fig. 3) and spin and energy (Fig. 4), for time-evolution from domain wall initial conditions at the isotropic point, $\Delta = 1$, of the XXZ chain.

Exact spin, energy and entanglement entropy profiles for single spin-flip initial conditions

Following the analysis of Refs. [27, 43], the exact space-time profiles of spin, energy and entanglement for the initial condition

$$|\psi\rangle = |\uparrow\rangle^{\otimes L/2-1} \otimes |\downarrow\rangle \otimes |\uparrow\rangle^{\otimes L/2}, \quad (14)$$

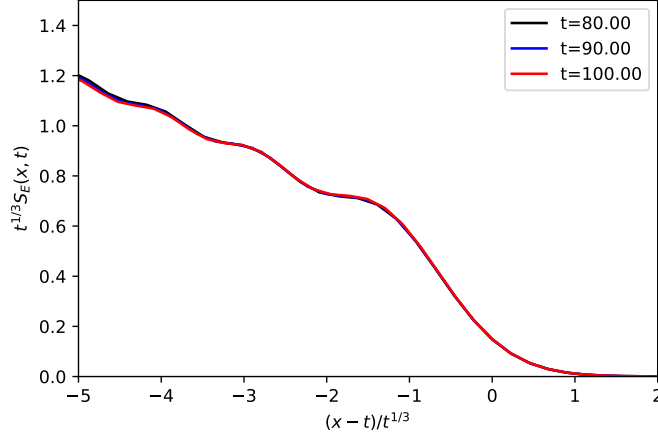


FIG. 3. Subdiffusive scaling collapse of fronts of single-cut entanglement entropy, obtained from tDMRG simulations of time-evolution from domain wall initial conditions in the XXZ chain, at anisotropy $\Delta = 1$.

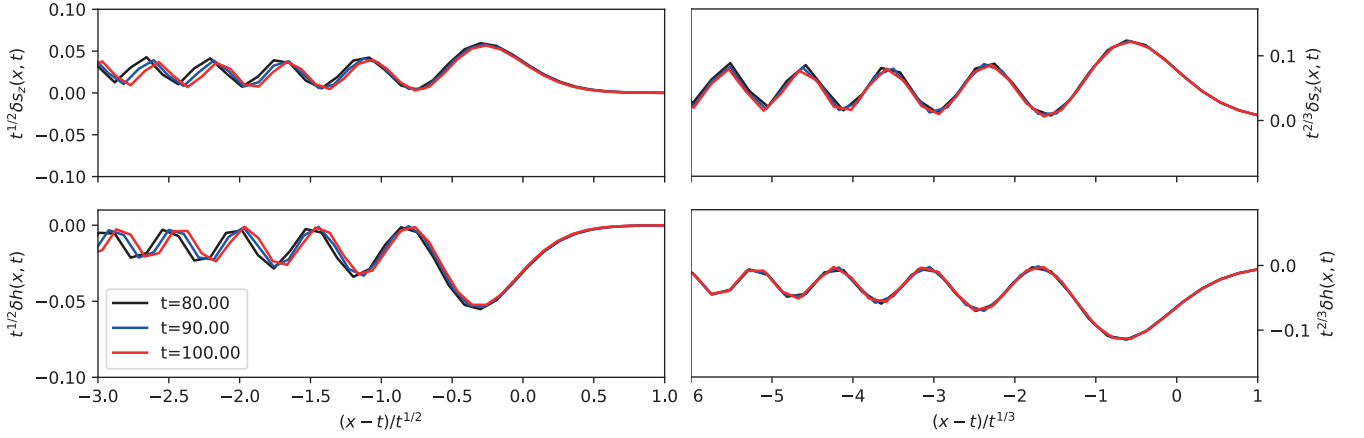


FIG. 4. Diffusive (*left*) versus subdiffusive (*right*) rescaling of fronts of spin (*top*) and energy (*bottom*), obtained from tDMRG predictions for time-evolution from domain wall initial conditions in the XXZ chain, at anisotropy $\Delta = 1$.

in the limit $L \rightarrow \infty$ are straightforwardly found to be

$$\begin{aligned}
 \langle S_n^z \rangle(t) &= \frac{1}{2} - J_n^2(t), \\
 \langle h_n \rangle(t) &= \frac{J\Delta}{4} - \frac{J\Delta}{2} (J_n^2(t) + J_{n+1}^2(t)), \\
 S_E(n, t) &= - \left(\sum_{m=-\infty}^n J_m^2(t) \right) \log \left(\sum_{m=-\infty}^n J_m^2(t) \right) - \left(\sum_{m=n+1}^{\infty} J_m^2(t) \right) \log \left(\sum_{m=n+1}^{\infty} J_m^2(t) \right), \quad (15)
 \end{aligned}$$

where the $J_m(t)$ denote Bessel functions of the first kind. Passing to the ballistic scaling limit, these become

$$\begin{aligned}
 S^z(x, t) &= \frac{1}{2} - \frac{1}{\pi} \frac{1}{t} \frac{1}{\sqrt{1 - (x/t)^2}}, \\
 h(x, t) &= \frac{J\Delta}{4} - \frac{J\Delta}{\pi} \frac{1}{t} \frac{1}{\sqrt{1 - (x/t)^2}}, \\
 S_E(x, t) &= - \left(\frac{1}{2} - \frac{1}{\pi} \sin^{-1} \left(\frac{x}{t} \right) \right) \log \left(\frac{1}{2} - \frac{1}{\pi} \sin^{-1} \left(\frac{x}{t} \right) \right) - \left(\frac{1}{2} + \frac{1}{\pi} \sin^{-1} \left(\frac{x}{t} \right) \right) \log \left(\frac{1}{2} + \frac{1}{\pi} \sin^{-1} \left(\frac{x}{t} \right) \right). \quad (16)
 \end{aligned}$$

The first two formulae can be obtained directly from considering the hydrodynamic time evolution of the initial state $\rho_k(x, 0) = \delta(x)$. The comparison of the ballistic approximation with numerical results and the exact time-evolution is

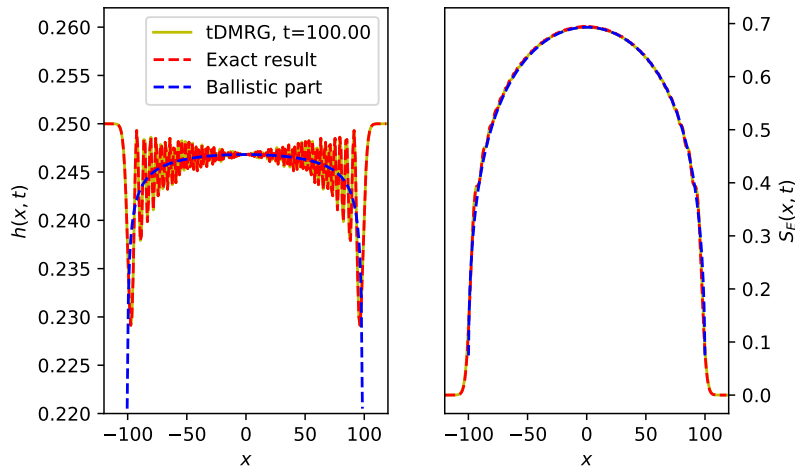


FIG. 5. *Left*: Energy profile at $t = 100$ obtained from tDMRG data for time-evolution from the initial condition Eq. (14), in the spin-1/2 XXZ chain with anisotropy $\Delta = 1$. The exact result Eq. (15) (red dash) is qualitatively very different from its ballistic part, Eq. (16) (blue dash) *Right*: The same plot but for single-cut entanglement entropy. The three curves are almost indistinguishable.

shown in Fig. (5). While the agreement for entanglement entropy is very good, the ballistic part of energy captures only the smoothed out profile, and the qualitative difference induced by third-order hydrodynamic effects is marked.

We now turn to the features that evolution from spin flips has in common with evolution from domain walls in the XXZ chain. For spin-flip initial conditions, the entanglement entropy does not exhibit the $t^{-1/3}$ height characteristic of entanglement spreading from domain walls²⁹. However, for both spin-flips and domain walls, fronts of spin and energy exhibit the same $t^{-2/3}$ height. In the context of spin flips, this follows directly from Bessel function asymptotics in the transitional region²⁷, which yield the front scaling

$$\delta s^z(x, t) \sim t^{-2/3} g_1\left(\frac{x-t}{t^{1/3}}\right), \quad \delta h(x, t) \sim t^{-2/3} g_2\left(\frac{x+0.5-t}{t^{1/3}}\right), \quad (17)$$

where $\delta s^z(x, t) = \langle s^z \rangle(x, t) - 1/2$, $\delta h(x, t) = \langle h \rangle(x, t) - J\Delta/4$ and

$$g_1(y) = -2^{2/3}[\text{Ai}(2^{1/3}y)]^2, \quad g_2(y) = -J\Delta 2^{2/3}[\text{Ai}(2^{1/3}y)]^2. \quad (18)$$

Here $\text{Ai}(z)$ denotes the Airy function (the offset in the energy front is a transient due to the local Hamiltonian being a two-site operator, that is nevertheless necessary to obtain a good agreement with analytics). See Fig. 6 for a late-time comparison with these predictions at $\Delta = 1$.

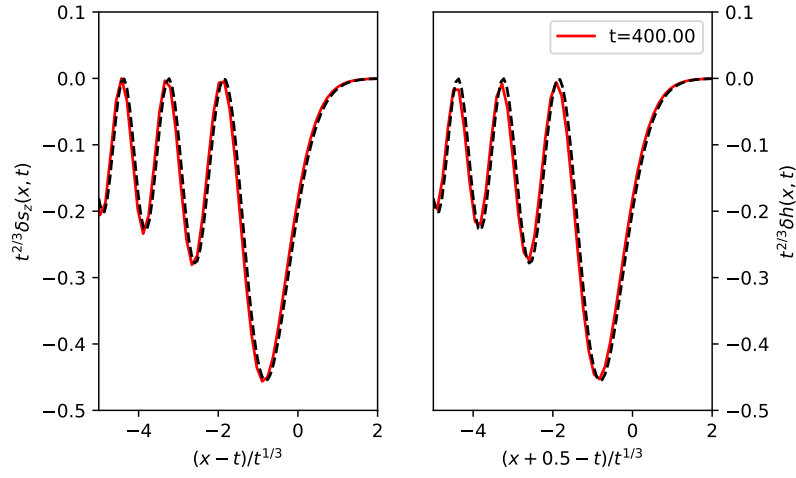


FIG. 6. Scaling collapse of fronts of spin and energy at $t = 400$, obtained from tDMRG data for time-evolution from the initial condition Eq. (14), in the spin-1/2 XXZ chain with anisotropy $\Delta = 1$. Exact asymptotic predictions (Eq. (17)) are dashed.